



## Phosphate adsorption using biochar derived from solid digestate

Diana Rodríguez Alberto <sup>a</sup>, Anna Christina Tyler <sup>b</sup>, Thomas A. Trabold <sup>a,\*</sup>

<sup>a</sup> Golisano Institute for Sustainability, Rochester Institute of Technology, Rochester, NY 14623, USA

<sup>b</sup> Thomas H. Gosnell School of Life Sciences, Rochester Institute of Technology, Rochester, NY 14623, USA

### ARTICLE INFO

**Keywords:**

Adsorption  
Anaerobic co-digestion  
Biochar  
Phosphate  
Thermochemical processes

### ABSTRACT

Anaerobic co-digestion of food waste and manure is an increasingly common waste management strategy. However, current disposal alternatives for the resulting effluent, "digestate", can lead to nutrient run-off and cause surface and groundwater contamination. Biochar made from the solid fraction of digestate was used to recover nutrients present in the liquid fraction of the same effluent stream. Biochar produced from solid digestate at three different temperatures (500, 800 and 1000 °C) was characterized and evaluated for adsorption of phosphate in solution and from liquid digestate. Pyrolysis temperature was negatively related to yield. However, higher processing temperatures (800 °C–1000 °C) are preferred due to better soil stability and phosphate adsorption capacity. Additional analysis to determine the potential to replicate this process at scale concluded that the amount of solid digestate biochar produced is sufficient to adsorb approximately 20% of the total phosphate present in the liquid fraction of the digestate.

### 1. Introduction

Food waste is a worldwide issue due to its impacts on the environment and the economy (Hall et al., 2009). It is estimated that 17% of the total global food production will go to waste (United Nations Environment Programme, 2021). In the United States, 40% of the food produced by restaurants, grocery stores, and households is not consumed by humans. This was approximately 6 million metric tons and \$161 billion worth of food in 2010 (USDA, 2014). Resources like fresh water and fossil fuels are consumed to produce food that will never be eaten. The majority of this food will reach the landfill, where it will decompose and emit methane and carbon dioxide, gases that contribute to climate change (Hall et al., 2009). In response to this issue, several pathways have emerged as an alternative to landfilling. These include repurposing food waste as animal feed or processing it through composting or wastewater treatment plants (Trabold and Nair, 2018). But there is particular interest in the valorization of food waste by turning it into energy products, like biogas, hydrogen, syngas or ethanol. This is known as the waste-to-energy pathway and includes processes like fermentation, anaerobic digestion and thermochemical conversion (Pham et al., 2015).

Anaerobic co-digestion is an established waste-to-energy process where microorganisms break down food waste in combination with animal manure in the absence of oxygen (Zhang et al., 2013). This

process results in two primary co-products: biogas and digestate. Biogas is a type of biofuel, mainly composed of methane and carbon dioxide, which once refined can be used for heating or electricity production (Mata-Alvarez et al., 2000). Digestate is the effluent from the digestion process which can be separated into its solid and liquid fractions. Liquid digestate is rich in nutrients like nitrogen, phosphorus, and potassium, and for this reason, it is often used on crop fields as an alternative to fertilizer (Möller and Müller, 2012). But there are some challenges associated with this practice. Field spreading of digestate requires the transportation of large volumes of the liquid by-product, which can become quite costly for the anaerobic digester operation (Armington, 2019). In addition, the tractors needed to survey the field to distribute the product contribute to soil compaction, which can affect crop yields (Verdi et al., 2019). There are also environmental risks associated with field spreading. One of them is the potential for nutrient pollution due to the excess nitrogen and phosphorus present in digestate, that can lead to nutrient run-off and consequently to the contamination of water resources (Shrestha, 2020).

Biochar is one of the products from thermochemical processing of biomass under low oxygen conditions. Traditionally this material has been used for soil improvement, due to its capacity to retain nutrients and water. In addition, its uniquely porous and high surface area properties make it suitable as an adsorption medium, comparable to activated carbon (Lehmann, 2007), and it can be applied to remove

\* Corresponding author.

E-mail address: [tatasp@rit.edu](mailto:tatasp@rit.edu) (T.A. Trabold).

pollutants from water and soil (Oliveira et al., 2017). In this work, we have assessed the option of producing biochar from the solid fraction of digestate, and then using this material to recover the nutrients present in the liquid digestate fraction. After the adsorption process, the now nutrient-rich biochar can be recovered and applied to fields as a solid fertilizer, thereby linking anaerobic co-digestion with thermochemical processing.

The integration of anaerobic digestion with thermochemical processing has been studied by several groups with the goal of making both systems more efficient from environmental and economic standpoints (e.g., Codignole Luz et al., 2018). Many of these studies have approached this integration with the goal of enhancing energy generation, which may be possible by taking advantage of the bio-oil and syngas energy products generated from thermochemical processing (Feng and Lin, 2017). However, in this study we focus solely on the production of biochar with the purpose of nutrient recovery and subsequent soil amendment.

Biochar has been made from a variety of anaerobically digested feedstock materials, including swine manure (Hung et al., 2017), dairy manure (Streibel et al., 2012) and food waste (Liu et al., 2020). However, to the best of our knowledge, the production of biochar from solid digestate resulting from the co-digestion of food waste and dairy manure has not been reported previously. The study of this combination is relevant when considering co-digestion as an alternative to food waste disposal, and because the characteristics of the feedstock are determining factors of the physical-chemical characteristics of the resulting biochar (Zhao et al., 2013). Another important factor that influences the characteristics of biochar is its processing temperature, and for this reason we assessed the production of biochar from digestate at three different temperatures. The characterization of the materials produced at different temperatures will inform selection of optimal conditions to obtain biochar with the characteristics required to serve as both adsorbent and soil amendment.

Nutrient recovery using biochar has been explored previously, often using woody biomass as the feedstock (Barber et al., 2018). Streibel et al. (2012) used biochar produced from anaerobically digested dairy manure to recover phosphorus from anaerobic digester effluent, through an experimental lagoon filtration system that used the synthesized biochar as the adsorption medium for 15 days. They found that around 30% of the phosphorus present in the effluent was recovered through this process, demonstrating the potential of biochar made from digested material as a medium for nutrient adsorption.

The objective of this study is to evaluate the effectiveness of using biochar, prepared at various temperatures from the solid digestate of a commercial co-digestion facility, to recover phosphate from the liquid fraction of the same digestate stream. We have selected phosphorus as our target nutrient because currently most of the phosphorus used in agriculture globally comes from non-renewable sources, therefore phosphorus recovery will be key to meeting the ever-growing agricultural fertilizer demand (Wang et al., 2017). In addition, phosphorus is the main nutrient responsible for the eutrophication of fresh water systems, therefore it is important to find ways to improve retention on agricultural fields (Correll, 1998).

To assess the suitability of biochar as a soil amendment, we performed a full characterization of the material based on the standard proposed by the International Biochar Initiative (IBI). For the evaluation of biochar as an adsorption medium, we produced biochar from solid digestate at three different temperatures (500, 800 and 1000 °C). Adsorption of phosphate was tested using a synthetic phosphate solution and as well as the effluent from the actual anaerobic co-digestion process. Finally, we assessed the capacity to scale this process for use at a commercial digester facility.

## 2. Materials and methods

### 2.1. Biochar preparation

Solid digestate used as the feedstock for biochar preparation was collected from an anaerobic digester located in Upstate New York. This facility processes cow manure along with industrial food waste in a 48% to 52% v/v ratio. After passing the digestate through a screw press to separate solid and liquid phases, the solid fraction was dried in an oven for at least 8 h at 105 °C.

Thermal processing was performed using a high-temperature furnace (CM Furnaces Inc., Bloomfield, New Jersey, USA). This instrument has a coupled microwave generator (SAIREM SAS) that was not employed in this study. Crucibles containing 10 to 20 g of previously dried samples were placed inside the furnace. Industrial grade nitrogen gas (AIRGAS CY-NI 300) was used to create an inert environment. Samples were processed at three different temperatures: 500 °C, 800 °C, and 1000 °C. The heating rate of 10 °C/min and residence time of 1 h at the desired temperature were kept constant for each of the tests. In each case, the furnace was cooled at a rate of between 5 and 6 °C/min, after the 1 h residence time. Due to limitations in the amount of material that could be processed at a time, the quantity of biochar needed for the analyses described below was generated by multiple runs of the furnace at each temperature.

Biochar yield was calculated based on Eq. (1) (Weber and Quicker, 2018):

$$\text{Mass yield (\%)} = \left[ \frac{W_b}{W_f} \right] \times 100 \quad (1)$$

where  $W_b$  represents the mass in grams of the biochar and  $W_f$  is the dry mass in grams of the feedstock. The effect of pyrolysis temperature on biochar yield was analyzed statistically using a one-way ANOVA with temperature as a fixed factor. Significant differences among means were determined with a Tukey HSD post hoc test in JMP Pro 15 statistical software.

### 2.2. Biochar characterization

#### 2.2.1. SEM Imaging

Images of the surface of biochar were captured using a Scanning Electron Microscope (SEM) (AMRAY 1830) coupled with an X-Ray Fluorescence System (IXRF Systems 550i). Biochar samples were attached to the sample holder using conductive carbon double-faced adhesive tape (Nissin EM Co., Ltd.).

#### 2.2.2. IBI standard characterization

The International Biochar Initiative (IBI) provides a standard group of characterization methods for biochar for use in soils. Since soil application is one of the proposed uses of our material, we subscribed to these guidelines. The IBI standard identifies three categories of testing for biochar materials: (1) basic utility properties, (2) assessment of potential toxicants and (3) solid enhancement properties (International Biochar Initiative, 2015).

Moisture, total ash, and volatile matter were determined using the ASTM D1762-84 Standard test method for chemical analysis of wood charcoal (ASTM, 2013). Elemental analysis (C, H, N) was performed using dry combustion following ASTM D4373-14 Standard test method for rapid determination of carbonate content of soils (ASTM, 2014). The sample pH, electrical conductivity and metal concentration were based on the Test Methods for Examination of Composting and Compost (USDA, 2001). Because of the rather high cost of the full IBI characterization, one biochar sample was analyzed for each of the three processing temperatures.

### 2.2.3. Surface area analysis

The surface area of biochar samples was measured by two different methods. Measurements using the butane activity correlation method were performed by a third-party laboratory based on ASTM D5742 - 95 Standard Test Method for Determination of Butane Activity of Activated Carbon (ASTM, 2006). For in-house analysis, we used the multi-point Brunauer–Emmett–Teller (BET) method for measurements of  $N_2$  adsorption at  $-196^\circ\text{C}$  (boiling point of liquid nitrogen) acquired using a Quantachrome Nova 4200e. Before each analysis, samples were dried under vacuum for 6 h at  $120^\circ\text{C}$  (Sigmund et al., 2017) and tested in quadruplicate.

### 2.3. Phosphate adsorption

We assessed the phosphate adsorption capacity of digestate biochar produced at 500, 800 and 1000  $^\circ\text{C}$ , and how it compares to commercially available wood biochar. The wood biochar was produced by the gasification of waste wood from shipping pallets at temperature around 500–600  $^\circ\text{C}$ . For the phosphate adsorption experiments, a stock solution of 200 mg  $\text{L}^{-1}$  (computed in mg  $\text{PO}_4^{3-}$ ) was prepared using potassium phosphate monobasic ( $\text{KH}_2\text{PO}_4$ ). Phosphate solutions for the experiments described below were then prepared by diluting the stock solution. For the adsorption of phosphate from liquid digestate, the digestate was first centrifuged at 4500 rpm for 30 min and filtered using 0.45  $\mu\text{m}$  PES membrane filters (Merck Millipore) to remove suspended solids. The starting concentration of the digestate was then determined using a spectrophotometer (Hach DR3900) and the Molybdo-Vanadate Method (Hach Method 10,214). Diluted liquid digestate samples were then prepared to match the concentrations used in the synthetic solution. Liquid digestate samples were collected during an 18-month period and characterized to determine its average composition (Table S1, Supplementary material).

Samples were prepared by adding 0.25 g of biochar to a 50 mL flask along with 25 mL of phosphate solution. Controls contained the same amounts of biochar and deionized water as the solution. The flasks were sealed and shaken at 100 rpm at room temperature for 24 h. The samples were transferred to a centrifuge tube and centrifuged at 4500 rpm for 30 min, and the resulting supernatant solution was filtered using 0.45  $\mu\text{m}$  PES membrane filters (Merck Millipore). Initial (solution only, no biochar) and final concentrations were determined using a spectrophotometer as described above. All adsorption experiments were conducted in triplicate.

The adsorption capacity at equilibrium ( $q_e$ , mg/g) and removal efficiency ( $R$ , %) were determined using Eqs. (2) and (3) (Kizito et al., 2017):

$$q_e = \frac{(C_o - C_e)V}{m} \quad (2)$$

$$R = \frac{(C_o - C_e)}{C_o} \times 100 \quad (3)$$

where  $C_o$  (mg  $\text{L}^{-1}$ ) denotes the initial phosphate concentration;  $C_e$  (mg  $\text{L}^{-1}$ ) denotes phosphate concentration at equilibrium;  $V$  (L) is solution volume;  $m$  (g) is adsorbent mass. The effect of pyrolysis temperature on removal efficiency was analyzed statistically using a mixed generalized regression with pyrolysis temperature as a fixed factor and initial solution concentration as a continuous factor in JMP Pro 15 statistical analysis software. The phosphate adsorption capacity of the digestate biochar was compared to activated carbon (AC) data found in the literature (Shi et al., 2011).

### 2.4. Isotherm modeling

The experimental data were analyzed using the Freundlich and Langmuir adsorption isotherms. The isotherm modeling was performed

using Microsoft Excel with the SOLVER function (Hossain et al., 2013). The Freundlich equation can be represented as:

$$q_e = KC_e^{\left(\frac{1}{n}\right)} \quad (4)$$

where  $C_e$  is the equilibrium concentration of phosphate and  $K$  and  $n$  are constants for a given adsorbate and adsorbent at a given temperature (Chen, 2015). Alternatively, the Langmuir isotherm is expressed in the following form:

$$q_e = q_m K_L \frac{C_e}{1 + K_L C_e} \quad (5)$$

where  $C_e$  is the concentration of phosphate solution at equilibrium and  $q_m$  and  $K_L$  are constants related to adsorption capacity and energy or net enthalpy of adsorption, respectively (Chen, 2015).

## 3. Results and discussion

### 3.1. Digestate biochar characterization

SEM images of the surface of digestate biochar show distinct differences among samples processed at different temperatures (Fig. 1). The surface of the sample processed at 500  $^\circ\text{C}$  shows a well-defined fibrous structure that can be attributed to lignocellulose remaining in the biochar. This fibrous structure is less noticeable with increasing temperature, and at 1000  $^\circ\text{C}$  very little evidence of the original morphology is visible.

Fig. 2 presents the effects of temperature on the mass yield of the biochar obtained. It was expected that the yield would decrease with temperature, and there was a drop in yield from 500  $^\circ\text{C}$  to 800  $^\circ\text{C}$ , but yield at 800  $^\circ\text{C}$  and 1000  $^\circ\text{C}$  were similar ( $df = 2$ ,  $F = 85.3$ , and  $p < 0.0001$ ). This may be due to the lignin content of the feedstock which contributes to its stability. For both woody and non-woody biomass, yields vary most at low processing temperatures, but are only weakly temperature-dependent above 400  $^\circ\text{C}$  (Weber and Quicker, 2018).

The basic utility properties of biochar made from digestate at different temperatures and commercial wood biochar are presented in Table 1. The carbon stability of the biochar is represented by the molar ratio of hydrogen to organic carbon. Materials with  $\text{H:C}_{\text{org}}$  higher than 0.7 are considered not thermochemically altered or partially altered (International Biochar Initiative, 2015). The sample processed at 500  $^\circ\text{C}$  is near that upper limit with  $\text{H:C}_{\text{org}} = 0.66$ , while samples 800  $^\circ\text{C}$  and 1000  $^\circ\text{C}$  have significantly lower ratios of 0.28 and 0.16, respectively. Based on the organic carbon content the IBI separates biochar into different classes that relate to the material's stability in soil for 100 years, with higher values representing greater potential for long term storage in soil. The obtained biochar can be identified as Class 2 for the sample processed at 500  $^\circ\text{C}$ , and Class 4 for the samples processed 800  $^\circ\text{C}$  and 1000  $^\circ\text{C}$ , suggesting that the higher processing temperature will lead to persistence in the soil and greater potential for soil enhancement (International Biochar Initiative, 2015). The basic utility values for biochar were similar to biochar derived from wood pallets (Table 1) for most properties, except for higher ash and nitrogen content in digestate-derived biochar.

Since the feedstock used in the production of this biochar is derived from a wide variety of sources, there is a risk of the presence of toxicants found in feedstock material such as heavy metals and polychlorinated biphenyls (International Biochar Initiative, 2015). All metals evaluated were within the maximum allowed thresholds proposed by the IBI (Table 2). Iron content of digestate biochar is relatively high (10,760–11,805 mg/kg) when compared to commercial wood biochar and other similar materials like dairy manure biochar (2290 mg/kg, for biochar produced at 700  $^\circ\text{C}$ ) (Cantrell et al., 2012). This unexpected characteristic of the material is linked to its magnetic properties. Normally, magnetic biochar is obtained by treating the feedstock with ferric

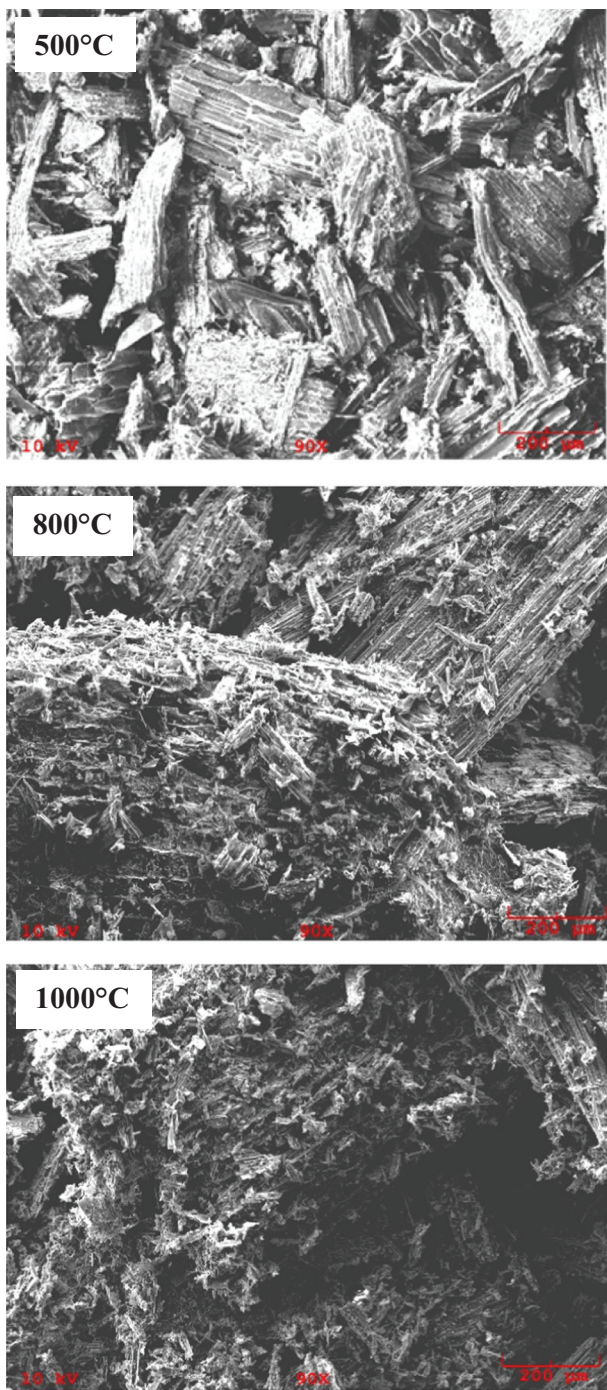


**Fig. 1.** Scanning electron microscopy (SEM) images of digestate biochar produced at different temperatures. Magnification: 90×. Scale: 200  $\mu\text{m}$ .

salt or some other iron-containing compound before going through thermochemical processing (Thines et al., 2017), but in this case, it was obtained without the addition of any precursor. This can be explained by the relatively high iron content ( $\sim 8000 \text{ mg L}^{-1}$ ) naturally present in the solid digestate (D. Rodríguez Alberto et al., 2019). Aside from the significant differences in iron content between the digestate biochar samples and commercial wood biochar, there are also relatively large variations in chlorine and sodium content. Whereas wood biochar had chlorine content of 1027 mg/kg vs. 189 mg/kg for digestate biochar produced at the same temperature, wood biochar had no detectable sodium compared to greater than 4000 mg/kg for all three digestate biochar samples.

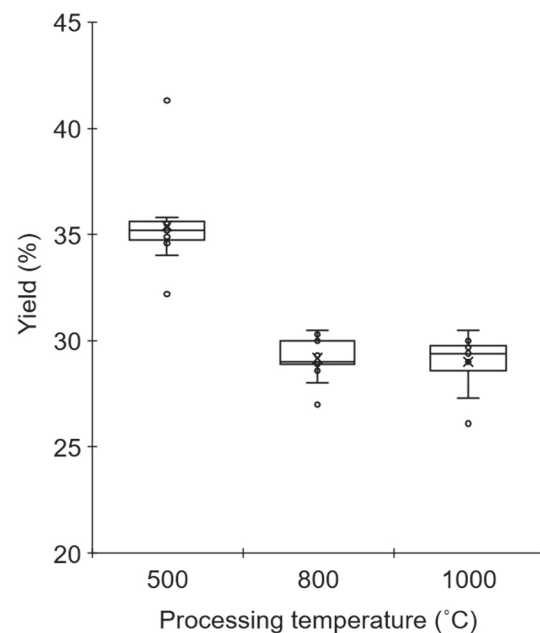


**Fig. 2.** Box plot summary of the effects of temperature on the mass yield of digestate biochar. “X” represents the mean value.

**Table 1**  
Basic utility properties of digestate biochar.

| Parameter               | 500 °C | 800 °C | 1000 °C | Wood biochar | Units              |
|-------------------------|--------|--------|---------|--------------|--------------------|
| Moisture                | 4.2    | 3.0    | 2.0     | 2.7          | % wet wt.          |
| Organic carbon          | 71.2   | 78.9   | 81.8    | 88.7         | % dry wt.          |
| H:C <sub>org</sub>      | 0.66   | 0.28   | 0.16    | 0.39         | Molar Ratio        |
| Total ash               | 12.4   | 13.7   | 14.4    | 2.7          | % dry wt.          |
| Total nitrogen          | 1.99   | 1.66   | 1.41    | 1.09         | % dry wt.          |
| pH                      | 9.45   | 11.17  | 11.29   | 9.86         | pH                 |
| Electrical conductivity | 0.264  | 1.427  | 1.913   | 0.426        | dS/m               |
| Liming                  | 9.7    | 11.4   | 12.4    | 5.5          | %CaCO <sub>3</sub> |

**Table 2**  
Metal content of digestate biochar.

| Parameter (mg/kg) | 500 °C | 800 °C | 1000 °C | Wood biochar | Max. allowed thresholds |
|-------------------|--------|--------|---------|--------------|-------------------------|
| Arsenic (As)      | ND     | ND     | ND      | 1.8          | 13–100                  |
| Cadmium (Cd)      | ND     | ND     | ND      | ND           | 1.4–39                  |
| Chromium (Cr)     | 9.9    | 6.7    | 9.6     | 4.0          | 93–1200                 |
| Cobalt (Co)       | 3.1    | 2.6    | 3.8     | ND           | 34–100                  |
| Copper (Cu)       | 166    | 154    | 231     | 103          | 143–6000                |
| Lead (Pb)         | 3.2    | 0.3    | ND      | 2.8          | 121–300                 |
| Mercury (Hg)      | ND     | ND     | ND      | ND           | 1–17                    |
| Molybdenum (Mo)   | 3.8    | 2.1    | 2.9     | 1.2          | 5–75                    |
| Nickel (Ni)       | 4.8    | 3.6    | 4.8     | 2.0          | 47–420                  |
| Selenium (Se)     | ND     | ND     | ND      | ND           | 2–200                   |
| Zinc (Zn)         | 230    | 18.9   | ND      | 99.6         | 416–7400                |
| Boron (B)         | 43.8   | 42.7   | 38.1    | 21.1         | NS                      |
| Chlorine (Cl)     | 189    | 645    | 116     | 1027         | NS                      |
| Sodium (Na)       | 4087   | 4666   | 4176    | ND           | NS                      |
| Manganese (Mn)    | 167    | 157    | 163     | 174          | NS                      |
| Iron (Fe)         | 11,413 | 10,760 | 11,805  | 1302         | NS                      |

NS=non-specified. ND=non-detected.

Other types of toxicants that might be present in biochar are those that are produced during the thermochemical conversion process used to produce biochar, including polycyclic aromatic hydrocarbons (PAHs), dioxins and furans. Since these biochars were produced from slow pyrolysis (10 °C/min), which has been determined to produce a lower concentration of PAHs (Wang et al., 2017), we believe that the potential of PAH contamination is low. In addition, Weidemann et al. (2018) analyzed the concentration of PAHs, oxygenated polycyclic aromatic hydrocarbons (oxy-PAHs), nitrogen-containing polycyclic aromatic compounds (N-PACs), polychlorinated dibenz-p-dioxins (PCDDs), and dibenzofurans (PCDFs) in biochars produced from three different feedstocks, including anaerobic digestate, and determined that all samples were within the IBI's proposed limits and therefore suitable for soil application.

The soil enhancement properties of the biochar (Table 3) refer to the nutrients present in the material. The NPK of digestate biochar was compared to dairy manure, a common organic fertilizer. Pituello et al. (2015) reported the nutrient content of dairy manure, with N concentration of 1.7% calculated on a dry basis, P concentration of 4500 mg/kg, and a K value of 8800 mg/kg. When comparing dairy manure to digestate biochar at all processing temperatures, biochar shows a higher concentration of P, while the N and K values are in similar ranges to the ones found in manure. Further research is needed to determine the bioavailability of these nutrients (Chan and Xu, 2009).

Surface area measured using BET with N<sub>2</sub> adsorption was lower than results from the butane activity method. Since the produced material is highly porous and the diffusion rate of nitrogen molecules into micropores at -196 °C extremely low, these pores may be practically inaccessible to N<sub>2</sub> molecules (McLaughlin et al., 2012). In addition, another determining interference factor, especially for the biochar produced at 500 °C, is the possible presence of residual bio-oil and mobile matter residing in micropores. A better option for measuring surface area of this type of material is the use of CO<sub>2</sub> at 0 °C. At this higher temperature, it is possible to avoid diffusion limitations, and the physical properties of CO<sub>2</sub> make it possible to reach very low relative pressures (Garrido et al., 1987). Butane activity can be a viable indicator of the surface area trend when CO<sub>2</sub> adsorption is not an option (we do not have in-house capability and 3rd-party analysis is very expensive), but due to the fact that a significant portion of butane's adsorption capacity is at a low adsorption energy, surface area values may be lower than actual (McLaughlin et al., 2012).

### 3.2. Phosphate adsorption

The phosphate adsorption capacity and removal efficiency of digestate biochar varied substantially across production temperatures (Fig. 3). Regression analysis for removal efficiency yielded significant effects of concentration ( $F = 32.9$ ,  $p < 0.0001$ ,  $df = 1$ ), production temperature ( $F = 990.4$ ,  $p < 0.0001$ ,  $df = 2$ ), and their interaction ( $F = 21.4$ ,  $p < 0.0001$ ,  $df = 2$ ). Samples produced at 500 °C demonstrated no phosphate removal, and negative values indicating that phosphorous was leaching from the biochar material into the solution. At production temperatures of 800 °C and 1000 °C, the removal efficiency decreased

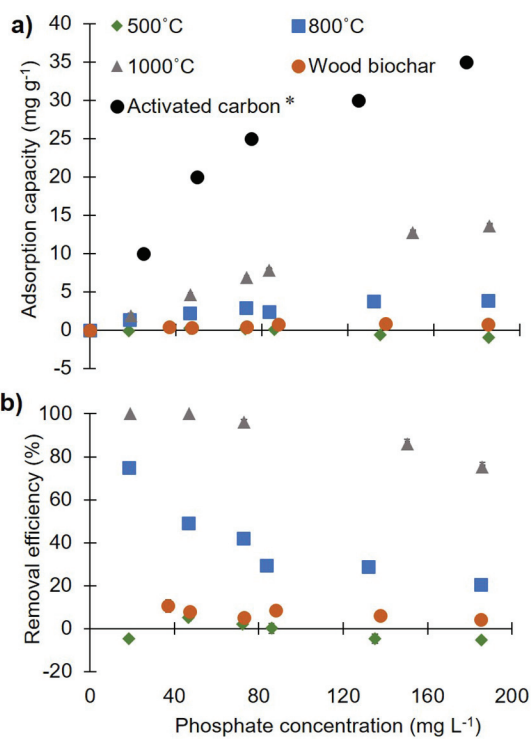


Fig. 3. Phosphate adsorption using digestate biochar prepared at different temperatures compared to commercially available wood biochar. (a) Adsorption capacity, also compared to activated carbon \*(Shi et al., 2011) (b) removal efficiency. Error bars represent standard error from the mean of triplicate experiments, in most cases not visible.

with increasing concentration, but at the higher concentrations, 1000 °C biochar significantly outperformed samples produced at both 500 °C and 800 °C. Biochar produced at 1000 °C provided 100% recovery of phosphate solution at 50 mg L<sup>-1</sup> or lower, dropping to about 75% at phosphate concentration of 180 mg L<sup>-1</sup>. Adsorption capacity with biochar produced at 800 °C was significantly lower, with removal efficiency of about 75% at 50 mg L<sup>-1</sup> and dropping to 25% when phosphate concentration increased to 180 mg L<sup>-1</sup>. The increasing adsorption capacity related to a higher processing temperature can be explained by the removal of carbon mass at higher temperatures which creates pores in the material, increasing its surface area and leading to higher removal (Trazzi et al., 2016).

Similar behavior was observed for both traditional and magnetic biochar made from orange peel, with the magnetic sample produced at a higher temperature demonstrating the highest adsorption capacity (Chen et al., 2011). This interaction between pyrolysis temperature and magnetic activity may be related to the form of iron oxide and its location in the composite (i.e., on the surface or embedded within the biochar) which is highly influenced by the processing temperature. In addition, there is a correlation between adsorption capacity and iron

Table 3  
Soil enhancement properties of digestate biochar.

| Parameter                       | 500 °C    | 800 °C      | 1000 °C     | Wood biochar | Units             |
|---------------------------------|-----------|-------------|-------------|--------------|-------------------|
| Ammonium (NH <sub>4</sub> -N)   | 12.2      | 7.8         | 7.8         | 3.7          | mg/kg dry wt.     |
| Nitrate (NO <sub>3</sub> -N)    | 0.8       | 0.7         | 3.1         | 1.4          | mg/kg dry wt.     |
| Phosphorus (P)                  | 13,730    | 11,790      | 11,376      | 1918         | mg/kg dry wt.     |
| Potassium (K)                   | 8677      | 10,318      | 12,256      | 3464         | mg/kg dry wt.     |
| Volatile matter                 | 30.6      | 19.5        | 18.4        | 7.7          | % dry wt.         |
| Surface area (butane activity)  | 205       | 203         | 172         | 288          | m <sup>2</sup> /g |
| Surface area (BET) <sup>a</sup> | 8.3 (3.4) | 173.1 (5.5) | 25.8 (4.25) | -            | m <sup>2</sup> /g |

<sup>a</sup>  $n = 10$ , values in parentheses represent standard deviation.

content in the biochar surface, so at this higher temperature (1000 °C) there might be a greater proportion of magnetite left than biochar (Chen et al., 2011). The presence of metal oxides is associated with a higher phosphate adsorption that can be explained by the aqueous phosphate forming a surface deposit with the metallic oxide through hydrogen bonds or by forming precipitation through a chemical reaction and resulting in better adsorption capacity (Ajmal et al., 2020; Yao et al., 2011).

Commercial wood biochar produced by gasification at 500–600 °C had a lower adsorption capacity than biochar produced at 800 °C and 1000 °C, and a similar behavior to the digestate biochar produced at 500 °C. This may be associated with the lower processing temperature or the lack of electrostatic interaction between the woody biochar and the phosphate ion (Vikrant et al., 2018). The data for phosphate adsorption using activated carbon (AC) was extracted from a study by Shi et al. (2011). Although experimental conditions were slightly different (1 h exposure period versus our 24 h exposure period), this comparison allows evaluation of the performance of digestate-derived biochar to more conventional products. The adsorption capacity of activated carbon was more than double that of the digestate biochar for each given concentration. However, synthesizing AC is a more energy intensive procedure requiring the extra step of carbon dioxide or steam activation (Ahmed et al., 2019). In contrast, solid digestate is a valorized waste material that can likely be obtained at low cost. Our experiments demonstrate the utility of digestate biochar for phosphate removal without any further treatment. The adsorption of phosphate present in liquid digestate solution using solid digestate biochar produced at 1000 °C was similar to that achieved using synthetic solutions of equivalent concentrations (Fig. 4). Our results were also compared to previous research using anaerobically digested biomass to produce biochar and used for phosphate recovery (Table S2, Supplementary material), having in mind that the pyrolysis and adsorption parameters vary within these studies and thus direct comparison of results is difficult.

### 3.3. Isotherm modeling

Both nonlinear adsorption isotherm relationships (Eqs. (4) and (5)) for digestate biochar produced at 1000 °C and a synthetic solution or liquid digestate (Fig. 5) provide reasonably good representations of the empirical data. However, the plots and  $R^2$  values (Table 4) indicate that the Freundlich model provides a slightly better fit. This is congruent with biochar produced from a variety of other materials and used to recover phosphate, including magnetic wood biochar (Ajmal et al., 2020), dairy- manure biochar (Chen et al., 2011; Choi et al., 2019), and

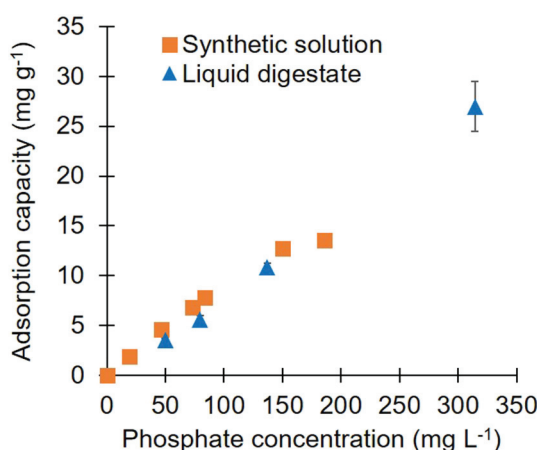


**Fig. 4.** Adsorption capacity of phosphate in liquid digestate solution vs synthetic solution using solid digestate biochar produced at 1000 °C. Error bars represent one standard deviation from the mean of triplicate experiments, in most cases not visible.

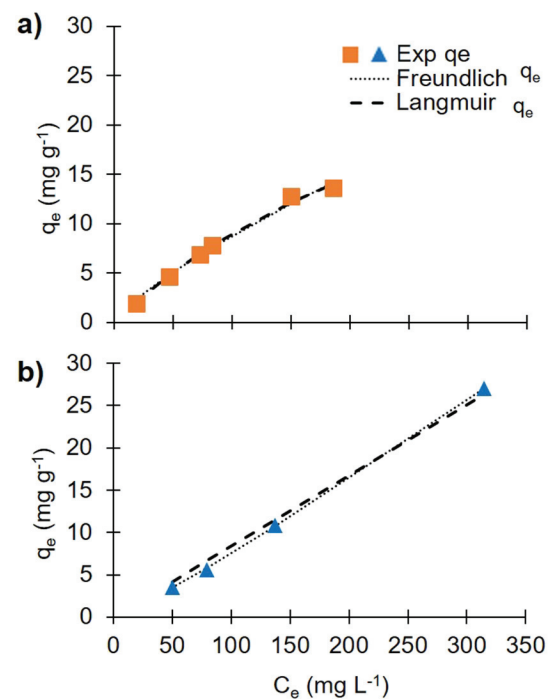


**Fig. 5.** Nonlinear fitting of Freundlich and Langmuir isotherm model using digestate biochar produced at 1000 °C as the adsorbent to recover phosphate from (a) synthetic solution and (b) liquid digestate.

**Table 4**

Isotherm constants for phosphate ion adsorption from two different sources.

| PO <sub>4</sub> source | Langmuir       |                |                | Freundlich |                |                |
|------------------------|----------------|----------------|----------------|------------|----------------|----------------|
|                        | q <sub>m</sub> | K <sub>L</sub> | R <sup>2</sup> | n          | K <sub>F</sub> | R <sup>2</sup> |
| Synthetic solution     | 39.72          | 0.003          | 0.9940         | 1.269      | 0.156          | 0.9880         |
| Liquid digestate       | 11,719         | 7.50E-07       | 0.9930         | 0.897      | 0.061          | 0.9998         |

digested sugar beet tailing biochar (Yao et al., 2011). The isotherm fitting to the Freundlich model can be an indication of a heterogeneous surface that can lead to a non-uniform sorption (Chen, 2015). However, as suggested by Vikrant et al. (2018), because the  $R^2$  values for the Langmuir and Freundlich isotherm model fits were found to be very close, it is reasonable to conclude that phosphate adsorption by the food waste and manure co-digestate biochar used in this study could be controlled by multiple processes. Isolating the specific physiochemical adsorption mechanisms will be the focus of our future research.

### 4. Potential for commercial application

Based on the favorable experimental results presented in Section 3, we conducted additional analysis to determine if the digestate biochar adsorption method has the potential to be replicated at scale, based on a case study of a local dairy farm-based Aco-D facility that produces 98,000 t of digestate annually. This is the same facility where solid digestate was collected, which processes cow manure along with industrial food waste in a 48% v/v to 52% v/v ratio. We collected data on the characteristics of the digestate of this site on a bimonthly basis and determined that the average liquid digestate phosphate concentration is 438 mg L<sup>-1</sup> (Fig. S3, Supplementary material). For this concentration we used the Freundlich model fit to the experimental data (Fig. 5b) to extrapolate a corresponding adsorption capacity of 39 mg g<sup>-1</sup>. Using this information, total biochar needed (TBN) was calculated using Eq. (6):

$$TBN = [\text{PO}_4]_{\text{LD}} * \rho_{\text{LD}}^{-1} * D * F_{\text{LD}} * AC^{-1} \quad (6)$$

where:

TBN = Total biochar needed (t)

$[\text{PO}_4]_{\text{LD}}$  = Concentration of phosphorus in liquid digestate (mg L<sup>-1</sup>)

$\rho_{\text{LD}}$  = Density of liquid digestate (kg/L)

D = Total mass of digestate (t)

$F_{\text{LD}}$  = Fraction of liquid digestate (%)

AC = Adsorption capacity of solid digestate biochar at a given concentration (mg/g)

Assuming a density of 1 kg/L for liquid digestate, we determined that to recover 100% of the phosphate present in the liquid, 1067 t of solid digestate biochar would be needed. Then we calculated the amount of biochar that is possible to produce under the conditions of this anaerobic co-digestion plant using Eq. (7):

$$PBP = D * F_{\text{SD}} * (1 - M_{\text{SD}}) * Y \quad (7)$$

where:

PBP = Potential biochar production (t)

D = Total mass of digestate (t)

$F_{\text{SD}}$  = Fraction of solid digestate (%)

$M_{\text{SD}}$  = Moisture content of solid digestate (%)

Y = Biochar production yield (%)

For the 98,000 t of digestate produced by the studied digester, 3% of the material is in solid form and 97% is liquid form, with a solid fraction moisture content of 73% and a biochar production yield of 30%. Under these assumptions it is possible to produce 238 t of solid digestate biochar. This result, coupled with the computed TBN value of 1067 t, suggests that by using solid digestate only as the biochar feedstock it is possible to produce enough biochar to adsorb about 20% of the phosphate in the liquid fraction and thus the use of digestate alone does not fulfill the plant's biochar needs with the current configuration. This result is comparable to the findings from Streubel et al. (2012) who were able to recover 30% of the phosphate present in digester effluent using biochar made from anaerobic digester fiber at 500 °C, although the methods and scale of this particular study differ to those used in our study. Future research will include assessing the potential use of solid manure biochar as an adsorbent. Solid manure is an abundant material at an AD facility, it has a higher solids content than digestate (~6%), and may be separated prior to digestion to improve plant efficiency. Thus, depending on its adsorption capacity, it could potentially satisfy the biochar requirements to completely recover the phosphate found in liquid digestate. This configuration sustains the purpose of using ACo-D as a waste management alternative for the food industry and makes use of resources already available in the digester setting to recover nutrients from digester effluent.

## 5. Conclusion

This study demonstrated the potential of using digestate biochar to recover nutrients from digester effluent. The synthesized biochar can adsorb 20% of the phosphate present in liquid digestate. Further research should address some of the challenges that have not been included in this study, such as additional equipment associated with scale-up application, the inclusion of other nutrients like nitrogen and potassium to fully capitalize on the fertilizer value of the digestate, and the disposal strategy for the final liquid effluent resulting from the

adsorption process.

## CRediT authorship contribution statement

**Diana Rodríguez Alberto:** Methodology, Investigation, Writing – original draft. **Anna Christina Tyler:** Conceptualization, Methodology, Writing – review & editing. **Thomas A. Trabold:** Conceptualization, Writing – review & editing, Supervision.

## Declaration of competing interest

The authors declare that they have no known competing financial interests or personal relationships that could have appeared to influence the work reported in this paper.

## Acknowledgments

This work was supported by the Golisano Institute for Sustainability and the National Science Foundation under Grant INFEWS CBET-1639391 that provided a graduate research assistantship for D. Rodríguez Alberto.

## Appendix A. Supplementary data

Supplementary data to this article can be found online at <https://doi.org/10.1016/j.biteb.2021.100864>.

## References

Ahmed, M.B., Hasan Johir, M.A., Zhou, J.L., Ngo, H.H., Nghiem, L.D., Richardson, C., Moni, M.A., Bryant, M.R., 2019. Activated carbon preparation from biomass feedstock: clean production and carbon dioxide adsorption. *J. Clean. Prod.* 225, 405–413. <https://doi.org/10.1016/j.jclepro.2019.03.342>.

Ajmal, Z., Muhammed, A., Dong, R., Wu, S., 2020. Probing the efficiency of magnetically modified biomass-derived biochar for effective phosphate removal. *J. Environ. Manag.* 253, 109730 <https://doi.org/10.1016/j.jenvman.2019.109730>.

Armington, W.R., 2019. *Food Waste Management Networks: Novel Methods for Overcoming Emerging Logistics Challenges*. Rochester Institute of Technology.

ASTM, 2006. Standard Test Method for Determination of Butane Activity of Activated Carbon. ASTM International. <https://doi.org/10.1520/D5742-16.2>.

ASTM, 2013. *ASTM D1762-84 Standard Test Method for Chemical Analysis of Wood Charcoal*.

ASTM, 2014. *ASTM D4373-14 Standard Test Method for Rapid Determination of Carbonate Content of Soils*.

Barber, S.T., Yin, J., Draper, K., Trabold, T.A., 2018. Closing nutrient cycles with biochar- from filtration to fertilizer. *J. Clean. Prod.* 197, 1597–1606. <https://doi.org/10.1016/j.jclepro.2018.06.136>.

Cantrell, K.B., Hunt, P.G., Uchimiyama, M., Novak, J.M., Ro, K.S., 2012. Impact of pyrolysis temperature and manure source on physicochemical characteristics of biochar. *Bioresour. Technol.* 107, 419–428. <https://doi.org/10.1016/j.biortech.2011.11.084>.

Chan, K.Y., Xu, Z., 2009. Biochar: nutrient properties and their enhancement. In: *EarthscanBiochar for Environmental Management: Science and Technology*, pp. 67–81. <https://doi.org/10.1002/qua.560260520>.

Chen, X., 2015. Modeling of experimental adsorption isotherm data. *Information* 6, 14–22. <https://doi.org/10.3390/info6010014>.

Chen, B., Chen, Z., Lv, S., 2011. A novel magnetic biochar efficiently sorbs organic pollutants and phosphate. *Bioresour. Technol.* 102, 716–723. <https://doi.org/10.1016/j.biortech.2010.08.067>.

Choi, Y.K., Jang, H.M., Kan, E., Wallace, A.R., Sun, W., 2019. Adsorption of phosphate in water on a novel calcium hydroxide-coated dairy manure-derived biochar. *Environ. Eng. Res.* 24, 434–442. <https://doi.org/10.4491/BER.2018.296>.

Codignole Luz, F., Cordiner, S., Manni, A., Mulone, V., Rocco, V., 2018. Biochar characteristics and early applications in anaerobic digestion-a review. *J. Environ. Chem. Eng.* 6, 2892–2909. <https://doi.org/10.1016/j.jece.2018.04.015>.

Correll, D.L., 1998. The role of phosphorus in the eutrophication of receiving waters: a review. *J. Environ. Qual.* 27, 261–266. <https://doi.org/10.2134/jeq1998.00472425002700020004x>.

Feng, Q., Lin, Y., 2017. Integrated processes of anaerobic digestion and pyrolysis for higher bioenergy recovery from lignocellulosic biomass: a brief review. *Renew. Sustain. Energy Rev.* 77, 1272–1287. <https://doi.org/10.1016/J.RSER.2017.03.022>.

Garrido, J., Linares-solano, A., Martín-Martínez, J.M., Molina-Sabio, M., Rodríguez-Reinoso, F., Torregrosa, R., 1987. Use of N2 vs: CO2 in the characterization of activated carbons. *Langmuir* 3, 76–81. <https://doi.org/10.1021/la00073a013>.

Hall, K.D., Guo, J., Dore, M., Chow, C.C., 2009. The progressive increase of food waste in America and its environmental impact. *PLoS One* 4, e7940. <https://doi.org/10.1371/journal.pone.0007940>.

Hossain, M., Ngo, H., Guo, W., 2013. Introductory of Microsoft Excel SOLVER function-Spreadsheet method for isotherm and kinetics modelling of metals biosorption in water and wastewater. *J. Water Sustain.* 3, 223–237.

Hung, C.-Y., Tsai, W.-T., Chen, J.-W., Lin, Y.-Q., Chang, Y.-M., 2017. Characterization of biochar prepared from biogas digestate. *Waste Manag.* 66, 53–60. <https://doi.org/10.1016/j.wasman.2017.04.034>.

International Biochar Initiative, 2015. Standardized product definition and product testing guidelines for biochar that is used in soil. *Int. Biochar Initiat.* 23 <https://doi.org/10.1016/j.zefq.2013.07.002>.

Kizito, S., Luo, H., Wu, S., Ajmal, Z., Lv, T., Dong, R., 2017. Phosphate recovery from liquid fraction of anaerobic digestate using four slow pyrolyzed biochars: dynamics of adsorption, desorption and regeneration. *J. Environ. Manag.* 201, 260–267. <https://doi.org/10.1016/j.jenvman.2017.06.057>.

Lehmann, J., 2007. Bio-energy in the black. *Front. Ecol. Environ.* 5, 381–387. [https://doi.org/10.1890/1540-9295\(2007\)5\[381:BITB\]2.0.CO;2](https://doi.org/10.1890/1540-9295(2007)5[381:BITB]2.0.CO;2).

Liu, J., Huang, S., Chen, K., Wang, T., Mei, M., Li, J., 2020. Preparation of biochar from food waste digestate: pyrolysis behavior and product properties. *Bioresour. Technol.* 302 <https://doi.org/10.1016/j.biortech.2020.122841>.

Mata-Alvarez, J., Macé, S., Llabrés, P., 2000. Anaerobic digestion of organic solid wastes. An overview of research achievements and perspectives. *Bioresour. Technol.* [https://doi.org/10.1016/S0960-8524\(00\)00023-7](https://doi.org/10.1016/S0960-8524(00)00023-7).

McLaughlin, H., Shields, F., Jagiello, J., Thiele, G., Services, M.A., 2012. *Analytical Options for Biochar Adsorption and Surface Area - Characterization of Biochar Materials*. North American Biochar Conference, Sonoma, CA, USA.

Möller, K., Müller, T., 2012. Effects of anaerobic digestion on digestate nutrient availability and crop growth: a review. *Eng. Life Sci.* 12, 242–257. <https://doi.org/10.1002/elsc.201100085>.

Oliveira, F.R., Patel, A.K., Jaisi, D.P., Adhikari, S., Lu, H., Khanal, S.K., 2017. Environmental application of biochar: current status and perspectives. *Bioresour. Technol.* 246, 110–122. <https://doi.org/10.1016/j.biortech.2017.08.122>.

Pham, T.P.T., Kaushik, R., Pashetti, G.K., Mahmood, R., Balasubramanian, R., 2015. Food waste-to-energy conversion technologies: current status and future directions. *Waste Manag.* 38, 399–408.

Pituello, C., Franciosi, O., Simonetti, G., Pisi, A., Torreggiani, A., Berti, A., Morari, F., 2015. Characterization of chemical–physical, structural and morphological properties of biochars from biowastes produced at different temperatures. *J. Soils Sediments* 15, 792–804. <https://doi.org/10.1007/s11368-014-0964-7>.

Rodriguez Alberto, D., Repa, K., Hegde, S., Miller, C.W., Trabold, T.A., 2019. Novel production of magnetite particles via thermochemical processing of digestate from manure and food waste. *IEEE Magn. Lett.* 10 <https://doi.org/10.1109/LMAG.2019.2931975>.

Shi, Z.L., Liu, F.M., Yao, S.H., 2011. Adsorptive removal of phosphate from aqueous solutions using activated carbon loaded with Fe(III) oxide. *Xinxing Tan Cailiao/New Carbon Mater* 26, 299–306. [https://doi.org/10.1016/S1872-5805\(11\)60083-8](https://doi.org/10.1016/S1872-5805(11)60083-8).

Shrestha, S., 2020. *Ecological Impacts of Food Waste Digestate Management in an Agricultural Watershed*. Rochester Institute of Technology.

Sigmund, G., Hüffer, T., Hofmann, T., Kah, M., 2017. Biochar total surface area and total pore volume determined by N2 and CO2 physisorption are strongly influenced by degassing temperature. *Sci. Total Environ.* 580, 770–775. <https://doi.org/10.1016/j.scitotenv.2016.12.023>.

Streubel, J.D., Collins, H.P., Tarara, J.M., Cochran, R.L., 2012. Biochar produced from anaerobically digested fiber reduces phosphorus in dairy lagoons. *J. Environ. Qual.* 41, 1166. <https://doi.org/10.2134/jeq2011.0131>.

Thines, K.R., Abdulla, E.C., Mubarak, N.M., Ruthiraan, M., 2017. Synthesis of magnetic biochar from agricultural waste biomass to enhancing route for waste water and polymer application: a review. *Renew. Sustain. Energy Rev.* 67, 257–276. <https://doi.org/10.1016/j.rser.2016.09.057>.

Trabold, T.A., Nair, V., 2018. *Conventional food waste management methods. In: Sustainable Food Waste-to-Energy Systems*.

Trazzi, P.A., Leahy, J.J., Hayes, M.H.B., Kwapiński, W., 2016. Adsorption and desorption of phosphate on biochars. *J. Environ. Chem. Eng.* 4, 37–46. <https://doi.org/10.1016/j.jece.2015.11.005>.

United Nations Environment Programme, 2021. *Food Waste Index Report 2021*. UNEP.

USDA, 2001. *Test Methods for the Examination of Composting and Compost (TMCC)*.

USDA, 2014. The estimated amount, value, and calories of postharvest food losses at the retail and consumer levels in the United States, EIB-121, U.S. Department of Agriculture, Economic Research Service. *SSRN Electron. J.* <https://doi.org/10.2139/ssrn.2501659>.

Verdi, L., Kuikman, P.J., Orlandini, S., Mancini, M., Napoli, M., Dalla Marta, A., 2019. Does the use of digestate to replace mineral fertilizers have less emissions of N2O and NH3? *Agric. For. Meteorol.* 269–270, 112–118. <https://doi.org/10.1016/J.AGRIFORMET.2019.02.004>.

Vikrant, K., Kim, K.H., Ok, Y.S., Tsang, D.C.W., Tsang, Y.F., Giri, B.S., Singh, R.S., 2018. Engineered/designer biochar for the removal of phosphate in water and wastewater. *Sci. Total Environ.* 616–617, 1242–1260. <https://doi.org/10.1016/j.scitotenv.2017.10.193>.

Wang, C., Wang, Y., Herath, H.M.S.K., 2017. Polycyclic aromatic hydrocarbons (PAHs) in biochar – their formation, occurrence and analysis: a review. *Org. Geochem.* 114, 1–11. <https://doi.org/10.1016/j.orggeochem.2017.09.001>.

Weber, K., Quicker, P., 2018. Properties of biochar. *Fuel* 217, 240–261. <https://doi.org/10.1016/j.fuel.2017.12.054>.

Weidemann, E., Buss, W., Edo, M., Mašek, O., Jansson, S., 2018. Influence of pyrolysis temperature and production unit on formation of selected PAHs, oxy-PAHs, N-PACs, PCDDs, and PCDFs in biochar—a screening study. *Environ. Sci. Pollut. Res.* 25, 3933–3940. <https://doi.org/10.1007/s11356-017-0612-z>.

Yao, Y., Gao, B., Inyang, M., Zimmerman, A.R., Cao, X., Pullammanappallil, P., Yang, L., 2011. Removal of phosphate from aqueous solution by biochar derived from anaerobically digested sugar beet tailings. *J. Hazard. Mater.* 190, 501–507. <https://doi.org/10.1016/j.jhazmat.2011.03.083>.

Zhang, C., Xiao, G., Peng, L., Su, H., Tan, T., 2013. The anaerobic co-digestion of food waste and cattle manure. *Bioresour. Technol.* 129, 170–176. <https://doi.org/10.1016/J.BIOTECH.2012.10.138>.

Zhao, L., Cao, X., Mašek, O., Zimmerman, A., 2013. Heterogeneity of biochar properties as a function of feedstock sources and production temperatures. *J. Hazard. Mater.* 256–257, 1–9. <https://doi.org/10.1016/j.jhazmat.2013.04.015>.